confirmed the close functionality of VAL1 and PHD-PRC2. *val1 vin3* and *val1 vrn2* plants were very delayed in flowering (Fig. 4D; table S6; and fig. S10, A to D) after 12 and 18 weeks of cold, and *FLC* expression remained high (fig. S10, E and F). This synergistic interaction is best explained by VAL1-VAL2 redundancy, with both proteins functioning through PHD-PRC2.

We propose that VAL1 binds sequence-specifically, probably as a homodimer, but potentially as a heterodimer with VAL2, to the RY motifs in the *FLC* nucleation region (Fig. 4E). This recruits the ASAP complex and potentially PRC1, resulting in the shutdown of transcription and reduced histone acetylation. In turn, these activities allow PHD-PRC2 nucleation and long-term epigenetic silencing of the locus. We cannot exclude the possibility of effects of VAL1 and VAL2 on *FLC* expression that are independent of the binding to *FLC* intron 1. The association of HDA19 with the PHD proteins suggests that it has multiple roles in the process, potentially interacting with VAL1 through SAP18 (*26*) for transcriptional repression and with VIN3 (and VRN5) to facilitate +1 nucleosome stabilization (*27*). It will now be important to investigate which components confer the switchlike on-off property that has been proposed for the nucleation event (*29*).

REFERENCES AND NOTES

1. S. D. Michaels, R. M. Amasino, *Plant Cell* **11**, 949–956 (1999).
2. C. C. Sheldon, D. T. Rouse, E. J. Finnegan, W. J. Peacock, E. S. Dennis, *Proc. Natl. Acad. Sci. U.S.A.* **97**, 3753–3758 (2000).
3. S. Swiezewski, F. Liu, A. Magusin, C. Dean, *Nature* **462**, 799–802 (2009).
4. S. Sung, R. M. Amasino, *Nature* **427**, 159–164 (2004).
5. T. Csorba, J. I. Questa, Q. Sun, C. Dean, *Proc. Natl. Acad. Sci. U.S.A.* **111**, 16160–16165 (2014).
6. M. Derkacheva, L. Hennig, *J. Exp. Bot.* **65**, 2769–2784 (2014).
7. A. R. Gendall, Y. Y. Levy, A. Wilson, C. Dean, *Cell* **107**, 525–535 (2001).
8. A. Angel, J. Song, C. Dean, M. Howard, *Nature* **476**, 105–108 (2011).
9. P. A. Steffen, L. Ringrose, *Nat. Rev. Mol. Cell Biol.* **15**, 340–356 (2014).
10. N. P. Blackledge, N. R. Rose, R. J. Klose, *Nat. Rev. Mol. Cell Biol.* **16**, 643–649 (2015).
11. B. Sun *et al.*, *Science* **343**, 1248559 (2014).
12. J. Mylne, T. Greb, C. Lister, C. Dean, *Cold Spring Harb. Symp. Quant. Biol.* **69**, 457–464 (2004).
13. K. Swaminathan, K. Peterson, T. Jack, *Trends Plant Sci.* **13**, 647–655 (2008).
14. H. Yang, M. Howard, C. Dean, *Curr. Biol.* **24**, 1793–1797 (2014).
15. M. Suzuki, H. H. Wang, D. R. McCarty, *Plant Physiol.* **143**, 902–911 (2007).
16. R. Nag, M. K. Maity, M. Dasgupta, *Plant Mol. Biol.* **59**, 821–838 (2005).
17. S. A. Braybrook *et al.*, *Proc. Natl. Acad. Sci. U.S.A.* **103**, 3468–3473 (2006).
18. W. Reidt *et al.*, *Plant J.* **21**, 401–408 (2000).
19. Y. Kagaya, K. Ohmiya, T. Hattori, *Nucleic Acids Res.* **27**, 470–478 (1999).
20. D. R. Boer *et al.*, *Cell* **156**, 577–589 (2014).
21. C. Schwerk *et al.*, *Mol. Cell. Biol.* **23**, 2981–2990 (2003).
22. C. Yang *et al.*, *Curr. Biol.* **23**, 1324–1329 (2013).
23. A. R. Pengelly, R. Kalb, K. Finkl, J. Müller, *Genes Dev.* **29**, 1487–1492 (2015).
24. N. J. Francis, R. E. Kingston, C. L. Woodcock, *Science* **306**, 1574–1577 (2004).
25. Y. Zhang, R. Iratni, H. Erdjument-Bromage, P. Tempst, D. Reinberg, *Cell* **89**, 357–364 (1997).
26. K. Hill, H. Wang, S. E. Perry, *Plant J.* **53**, 172–185 (2008).
27. E. Jean Finnegan, *Plant J.* **84**, 875–885 (2015).
28. K. K. Singh *et al.*, *RNA* **16**, 2442–2454 (2010).
29. A. Angel *et al.*, *Proc. Natl. Acad. Sci. U.S.A.* **112**, 4146–4151 (2015).

ACKNOWLEDGMENTS

We thank all members of the Dean and Howard research groups for discussions. We are grateful to G. Saalbach for assistance with mass spectrometry, M. Suzuki for providing *val1* and *val2* lines, J. Irwin for the *Brassica FLC* sequences, J. Long for the *hda19-1* line, and A. Pendle for the 35S::GFP-AtSAP18 plasmid. We thank V. Coustham, B. Rutjens, and J. Mylne for contributions at the early phase of this project. The Dean laboratory is supported by the UK Biotechnology and Biological Sciences Research Council and a European Research Council Advanced Investigator grant. The supplementary materials contain additional data.

SUPPLEMENTARY MATERIALS

www.sciencemag.org/content/353/6298/485/suppl/DC1
Materials and Methods
Figs. S1 to S10
Tables S1 to S7
References (*30*–*39*)

22 March 2016; accepted 1 July 2016
10.1126/science.aaf7354

SYMBIOSIS

Basidiomycete yeasts in the cortex of ascomycete macrolichens

Toby Spribille,[1,2]* Veera Tuovinen,[3,4] Philipp Resl,[1] Dan Vanderpool,[2] Heimo Wolinski,[5] M. Catherine Aime,[6] Kevin Schneider,[1]† Edith Stabentheiner,[1] Merje Toome-Heller,[6]‡ Göran Thor,[4] Helmut Mayrhofer,[1] Hanna Johannesson,[3] John P. McCutcheon[2,7]

For over 140 years, lichens have been regarded as a symbiosis between a single fungus, usually an ascomycete, and a photosynthesizing partner. Other fungi have long been known to occur as occasional parasites or endophytes, but the one lichen–one fungus paradigm has seldom been questioned. Here we show that many common lichens are composed of the known ascomycete, the photosynthesizing partner, and, unexpectedly, specific basidiomycete yeasts. These yeasts are embedded in the cortex, and their abundance correlates with previously unexplained variations in phenotype. Basidiomycete lineages maintain close associations with specific lichen species over large geographical distances and have been found on six continents. The structurally important lichen cortex, long treated as a zone of differentiated ascomycete cells, appears to consistently contain two unrelated fungi.

Most definitions of the lichen symbiosis emphasize its dual nature: the mutualism of a single fungus and single photosynthesizing symbiont, occasionally supplemented by a second photosynthesizing symbiont in modified structures (*1*–*4*). Together, these organisms form stratified, often leafy or shrubby body plans (thalli) that resemble none of the symbionts in isolation, a feature thought to be unique among symbioses (*1*). Attempts to synthesize lichen thalli from the accepted two components in axenic conditions, however, have seldom produced structures that resemble natural thalli (*5*, *6*). Notably, a critical structural feature of stratified lichens, the cortex, typically remains rudimentary in laboratory-generated symbioses (*5*). Recently, it has been suggested that microbial players, especially bacteria, may play a role in forming complete, functioning lichen thalli (*7*). However, although culturing and amplicon sequencing have revealed rich communities of microbes (*7*, *8*), including other fungi (*8*–*10*), no new stably associated symbiotic partners have been found.

The recalcitrance of lichens to form thalli in vitro means that characterizing symbiont gene activity (e.g., through transcriptomics) requires an approach that works with natural thalli. We used metatranscriptomics to better understand the factors involved in forming two macrolichen symbioses, *Bryoria fremontii* and *B. tortuosa*. These two species have been distinguished for 90 years by the thallus-wide production of the toxic substance vulpinic acid in *B. tortuosa*, causing it to appear yellowish, in contrast to *B. fremontii*, which is dark brown (*11*). Recent phylogenetic analyses have failed to detect any fixed sequence differences between the two species in either the mycobiont (Ascomycota, Lecanoromycetes, *Bryoria*) or the photobiont (Viridiplantae, *Trebouxia simplex*) when considering four and two loci, respectively (*12*, *13*). We hypothesized that differential gene expression might account for the

[1]Institute of Plant Sciences, NAWI Graz, University of Graz, 8010 Graz, Austria. [2]Division of Biological Sciences, University of Montana, Missoula, MT 59812, USA. [3]Department of Organismal Biology, Uppsala University, Norbyvägen 18D, 752 36 Uppsala, Sweden. [4]Department of Ecology, Swedish University of Agricultural Sciences, Post Office Box 7044, SE-75007 Uppsala, Sweden. [5]Institute of Molecular Biosciences, BioTechMed-Graz, University of Graz, 8010 Graz, Austria. [6]Department of Botany and Plant Pathology, Purdue University, West Lafayette, IN 47907, USA. [7]Program in Integrated Microbial Biodiversity, Canadian Institute for Advanced Research, Toronto, Ontario, Canada.
***Corresponding author. Email: toby.spribille@mso.umt.edu**
†Present address: Institute of Biodiversity, Animal Health and Comparative Medicine, College of Medical, Veterinary and Life Sciences, University of Glasgow, Glasgow G12 8QQ, UK. ‡Present address: Plant Health and Environmental Laboratory, Ministry for Primary Industries, Auckland, New Zealand.

Downloaded from http://science.sciencemag.org/ on August 31, 2016

increased production of vulpinic acid in *B. tortuosa*.

We first selected 15 thalli (six from *B. fremontii* and nine from *B. tortuosa*, all free from visible parasitic infection) from sites across western Montana, USA, for mRNA transcriptome sequencing. An initial transcriptome-wide analysis of single-nucleotide polymorphisms (SNPs) for Ascomycota and Viridiplantae transcript subsets showed no correlation between genotype and phenotype in *B. fremontii* and *B. tortuosa*, confirming previous results (*12*, *13*) (Fig. 1, A and B). Next, we estimated transcript abundances by mapping raw reads back to a single, pooled metatranscriptome assembly and binning by taxon. Restricting our analyses to Ascomycota and Viridiplantae revealed little differential transcript abundance associated with phenotype (Fig. 1, C and E). Taken together, these analyses confirm previous conclusions that the two lichen species are nomenclatural synonyms (*12*) but still provide no explanation for the underlying phenotypes (which we shall continue to refer to by their species names for convenience). However, by expanding the taxonomic range to consider all Fungi, we found 506 contigs with significantly higher abundances in vulpinic acid–rich *B. tortuosa* thalli. A majority of these contigs were annotated as Basidiomycota (Fig. 1D). These data suggested that a previously unrecognized basidiomycete was present in thalli of both species but was more abundant whenever vulpinic acid was present in large amounts.

We next sought to determine whether this uncharacterized basidiomycete was specific to the studied *Bryoria* species or could be found in other lichens. From metatranscriptome contigs containing ribosomal RNA (rRNA) basidiomycete sequences, we designed specific primers for ribosomal DNA [rDNA; 18*S*, internal transcribed spacer (ITS), and D1D2 domains of 28*S*) to screen lichens growing physically adjacent to *Bryoria* in Montana forests. Each assayed lichen species carried a genetically distinct strain of the basidiomycete, indicating a high degree of specificity. Furthermore, we found that *Letharia vulpina*, a common lichen species growing intermixed with *Bryoria*, maintained basidiomycete genotypes that were distinct from those in *Bryoria*, not only in Montana but also in northern Europe (fig. S1). When assaying for the basidiomycete across the seven main radiations of macrolichens in the class Lecanoromycetes, we found related basidiomycete lineages associated with 52 lichen genera from six continents, including in 42 of 56 sampled genera of the family Parmeliaceae (fig. S2). As a whole, these data indicate that basidiomycete fungi are ubiquitous and global associates of the world's most speciose radiation (*14*) of macrolichens.

To place the basidiomycete lineages in a phylogenetic context, we generated a 349-locus phylogenomic tree by using gene sequences inferred from our transcriptome data set and other available genomes (table S1). This analysis placed the basidiomycete as sister to *Cystobasidium minutum* (class Cystobasidiomycetes, subphylum Pucciniomycotina) with high support (Fig. 2A). The only previously known lichen-associated members of Cystobasidiomycetes are two species of *Cyphobasidium*, which is hypothesized to cause galls on species of Parmeliaceae (*15*). When incorporated into a broader sample of published cystobasidiomycete rDNA sequence data (*16*–*18*), the majority of our lichen-derived sequences form a strongly supported monophyletic clade with *Cyphobasidium* (Fig. 2B). Using current classification criteria (*18*), the lichen-associated lineages would include numerous new family-level lineages, and we recognize this set of subclades as the new order Cyphobasidiales (*19*). Applying a relaxed molecular clock to our phylogenomic tree

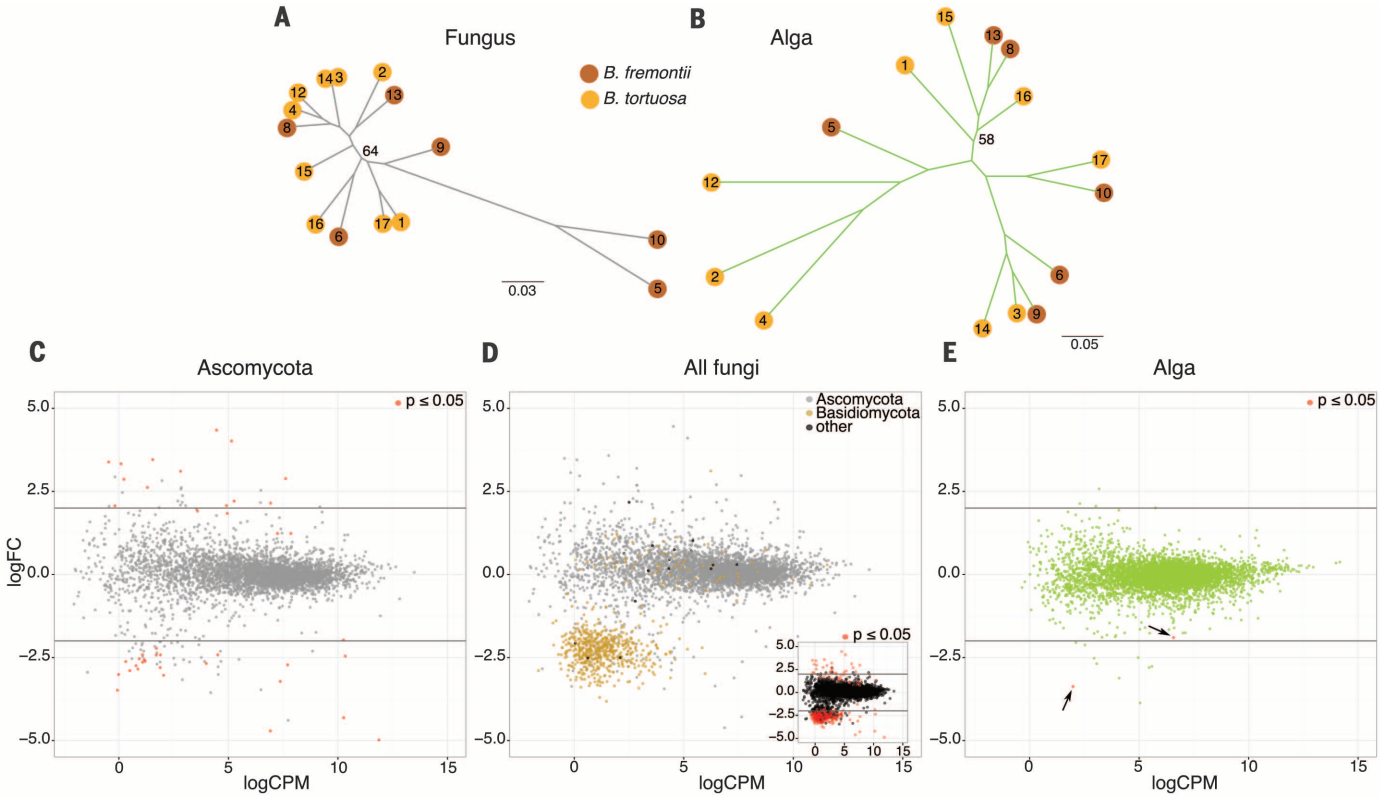

Fig. 1. Genome-wide divergence and transcript abundance of fungi and algae, based on symbiont subsets extracted from wild *Bryoria* metatranscriptomes. (**A** and **B**) Unrooted maximum likelihood topologies for (A) the Ascomycota member (lecanoromycete) and (B) the Viridiplantae member (alga) within the lichen pair *B. fremontii* and *B. tortuosa*, based on 30,001 and 25,788 SNPs, respectively. Numbers refer to metatranscriptome sample IDs (table S2). Scale bars indicate the average number of substitutions per site (**C** to **E**) Logarithm of the fold change (logFC) between vulpinic acid–deficient (*B. fremontii*) and vulpinic acid–rich (*B. tortuosa*) phenotypes in 15 *Bryoria* metatranscriptomes, plotted against transcript abundance (logCPM, logarithm of counts per million reads). Only transcripts found in all 15 samples were included. Ascomycota transcripts only are shown in (C). All fungal transcripts are shown in (D), with taxonomic assignments superimposed; a plot with statistically significant transcript differential abundance is shown as an inset. Viridiplantae transcripts are shown in (E). Red dots indicate a log fold change with $P < 0.05$ in (C), the inset of (D), and (E) (highlighted with arrows).

Downloaded from http://science.sciencemag.org/ on August 31, 2016

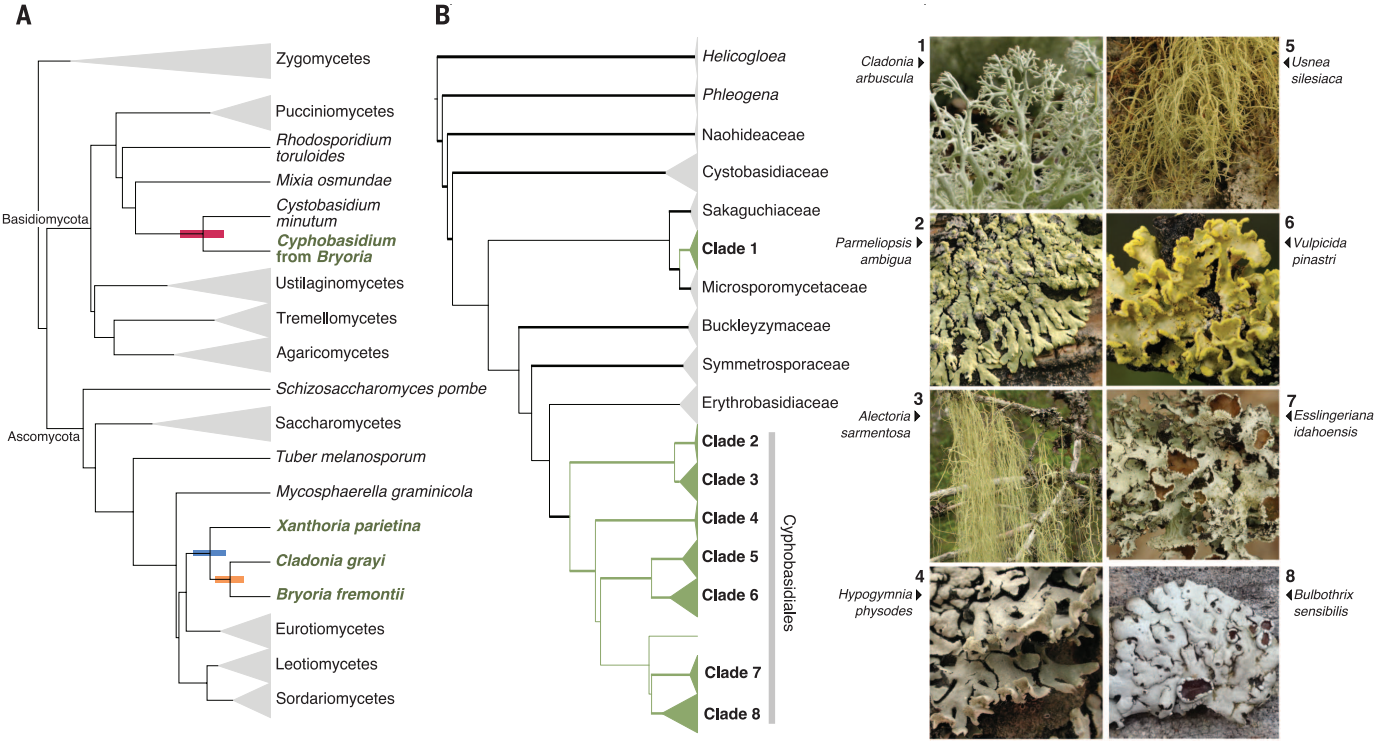

Fig. 2. Placement of Cyphobasidiales members and their diversity within lichens. (**A**) Maximum likelihood phylogenomic tree based on 39 fungal proteomes and 349 single-copy orthologous loci. Dating based on a 58-locus subsample shows relative splits between Cyphobasidiales and *Cystobasidium minutum* and splits leading to the lecanoromycete genera *Xanthoria*, *Cladonia*, and *Bryoria* (colored bars indicate 95% confidence intervals; fungi occurring in lichens are shown in green). (**B**) Maximum likelihood rDNA phylogeny of the class Cystobasidiomycetes, with images of representative lichen species from which sequences were obtained in each clade; thick branches indicate bootstrap support >70%. Shaded triangles are scaled to the earliest branch splits of underlying sequence divergence in each clade. Full versions of the trees are shown in fig. S3.

(Fig. 2A) shows the *Cystobasidium-Cyphobasidium* split occurring around the same time as the origin of three of the main groups of lecanoromycete macrolichens in which Cyphobasidiales species occur, suggesting a long, shared evolutionary history. Two fossil calibrations place this split at around 200 million years before the present (figs. S4 and S5).

Our initial microscopic imaging failed to reveal any cells that we could assign to Basidiomycetes with certainty. Furthermore, attempts to culture the basidiomycete from fresh thalli were unsuccessful. We therefore developed protocols for fluorescent in situ hybridization (FISH) targeting specific ascomycete and cystobasidiomycete rRNA sequences. Cystobasidiomycete-specific FISH probes unambiguously hybridized round, ~3- to 4-μm-diameter cells embedded in the peripheral cortex of both *B. fremontii* and *B. tortuosa* (Fig. 3 and movie S1). Consistent with the transcript abundance data, these cells were more abundant in thalli of *B. tortuosa* (Fig. 3), where they were embedded in secondary metabolite residues (movie S1). Imaging of other lichen species likewise revealed cells of similar morphology in the peripheral cortex (fig. S6). Composite three-dimensional FISH images from *B. capillaris* show the cells occurring in a zone exterior to the lecanoromycete (Fig. 4 and movie S2) and embedded in polysaccharides (Fig. 4C), explaining why these cells are not observed in scanning electron microscopy (Fig. 4A). In some species, such as *L. vulpina*, the abundance of hybridized living cells was low, but selective removal of the polysaccharide layer through washing revealed high densities of collapsed, apparently dead cells within the cortex (fig. S7). These dead cells may explain the paucity of the FISH signal in some experiments. The mononucleate single cells (fig. S8C), evidence of budding, and absence of hyphae or clamp connections are consistent with an anamorphic or yeast state in Cystobasidiomycetes. FISH imaging of *Cyphobasidium* galls on the lichen *Hypogymnia physodes*, obtained from Norway, confirmed the link to the sexual or teleomorphic state (fig. S8), which appears to develop rarely (*15*). These data suggest that the gall-inducing form of *Cyphobasidium* completes its life cycle entirely within lichens.

It is remarkable that *Cyphobasidium* yeasts have evaded detection in lichens until now, despite decades of molecular and microscopic studies of the Parmeliaceae (*20*–*22*). It seems likely that the failure to detect *Cyphobasidium* in both Sanger and amplicon sequencing studies (*8*) is due to multitemplate polymerase chain reaction bias. The most widespread clade of *Cyphobasidium* possesses a 595–base pair group I intron inserted downstream of the primer binding site ITS1F, doubling the template length of ITS, a popular fungal barcode (*23*). This, combined with low background abundance, can push a template below detection thresholds (*24*). Also, we cannot rule out that *Cyphobasidium* yeasts have actually been sequenced and discarded as presumed contaminants.

The lichen cortex layer has long been considered to be key for structural stabilization of macrolichens, as well as for water and nutrient transfer into the thallus interior (*6*, *25*). Most macrolichens possess a basic two-layer cortex scheme consisting of conglutinated internal hyphae and a thin, polysaccharide-rich peripheral layer (*25*). However, the internal cellular structure is not uniform across lichens (*26*), and the composition of extracellular polysaccharides is poorly known (*27*). In *Bryoria*, the layer in which *Cyphobasidium* yeasts occur has not been recognized as distinct from the cortex (*11*), although in other parmelioid lichens, a seemingly homologous layer has sometimes been referred to as the "epicortex" (*20*). The discovery of ubiquitous yeasts embedded in the cortex raises the prospect that more than one fungus may be involved in its construction, and it could explain why lichens synthesized in vitro from axenically grown ascomycete and algal cultures develop only rudimentary cortex layers (*5*).

In many lichens, the peripheral cortex layer in which *Cyphobasidium* yeasts are embedded is enriched with specific secondary metabolites (*25*), the production of which often does not correlate with the lecanoromycete phylogeny (*28*).

Downloaded from http://science.sciencemag.org/ on August 31, 2016

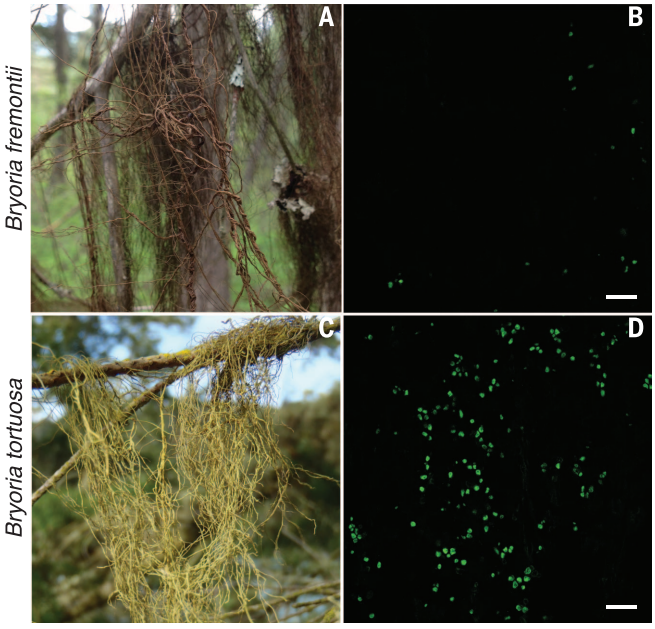

Fig. 3. Differential abundance of Cyphobasidiales yeasts in *B. fremontii* and *B. tortuosa*. (**A**) *B. fremontii*, with (**B**) few FISH-hybridized live yeast cells at the level of the cortex. (**C**) *B. tortuosa*, with (**D**) abundant FISH-hybridized cortical yeast cells (scale bars, 20 μm).

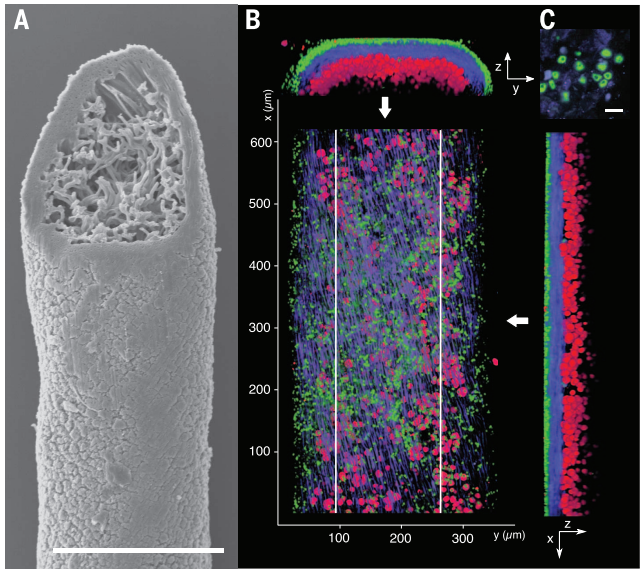

Fig. 4. Fluorescent cell imaging of dual fungal elements in lichen thalli. (**A**) Scanning electron microscopy image of a thallus filament of *B. capillaris* (scale bar, 200 μm). (**B**) FISH hybridization of *B. capillaris* thallus, showing Cyphobasidiales yeasts (green) and the lecanoromycete (blue) with algal chlorophyll A autofluorescence (red). The volume within the two vertical lines is visualized on the right; the unclipped frontal view is shown at the top. Movie S2 shows an animation of the three-dimensional ~100-μm z-stack. (**C**) Detail of yeast cells (scale bar, 5 μm).

The assumption that these substances are exclusively synthesized by the lecanoromycete must now be considered untested. In *B. tortuosa,* differential transcript and cell abundance data, along with physical adjacency to crystalline residues, implicate *Cyphobasidium* in the production of vulpinic acid, either directly or by inducing its synthesis by the lecanoromycete. Confirming a link by using transcriptome or genome data is impossible until the enzymatic synthesis pathway of vulpinic acid is described. However, related pulvinic acid derivatives are synthesized by other members of Basidiomycota (*29*).

The assumption that stratified lichens are constructed by a single fungus with differentiated cell types is so central to the definition of the lichen symbiosis that it has been codified into lichen nomenclature (*30*). This definition has brought order to the field but may also have constrained it by forcing untested assumptions about the true nature of the symbiosis. We suggest that the discovery of *Cyphobasidium* yeasts should change expectations about the potential diversity and ubiquity of organisms involved in one of the oldest known and most recognizable symbioses in science.

REFERENCES AND NOTES

1. A. De Bary, *Die Erscheinung der Symbiose* (Verlag Karl Trübner, 1879).
2. A. Gargas, P. T. DePriest, M. Grube, A. Tehler, *Science* **268**, 1492–1495 (1995).
3. F. Lutzoni, M. Pagel, V. Reeb, *Nature* **411**, 937–940 (2001).
4. D. L. Hawksworth, *Bot. J. Linn. Soc.* **96**, 3–20 (1988).
5. V. Ahmadjian, *The Lichen Symbiosis* (John Wiley & Sons, 1993).
6. R. Honegger, *New Phytol.* **125**, 659–677 (1993).
7. I. A. Aschenbrenner, T. Cernava, G. Berg, M. Grube, *Front. Microbiol.* **7**, 180 (2016).
8. S. T. Bates *et al.*, *Lichenologist* **44**, 137–146 (2012).
9. O. Petrini, U. Hake, M. M. Dreyfuss, *Mycologia* **82**, 444–451 (1990).
10. J. M. U'Ren, F. Lutzoni, J. Miadlikowska, A. E. Arnold, *Microb. Ecol.* **60**, 340–353 (2010).
11. I. M. Brodo, D. L. Hawksworth, *Opera Bot.* **42**, 1–164 (1977).
12. S. Velmala, L. Myllys, P. Halonen, T. Goward, T. Ahti, *Lichenologist* **41**, 231–242 (2009).
13. H. Lindgren *et al.*, *Lichenologist* **46**, 681–695 (2014).
14. G. Amo de Paz, P. Cubas, P. K. Divakar, H. T. Lumbsch, A. Crespo, *PLOS ONE* **6**, e28161 (2011).
15. A. M. Millanes, P. Diederich, M. Wedin, *Fungal Biol.* 10.1016/j.funbio.2015.12.003 (2015).
16. M. C. Aime *et al.*, *Mycologia* **98**, 896–905 (2006).
17. Q.-M. Wang *et al.*, *Stud. Mycol.* **81**, 27–53 (2015).
18. Q.-M. Wang *et al.*, *Stud. Mycol.* **81**, 149–189 (2015).
19. Cyphobasidiales T. Sprib. & H. Mayrhofer, ord. nov. (MB 816120); diagnosis is the same as type family Cyphobasidiaceae T. Sprib. & H. Mayrhofer, fam. nov. (MB 816119); embedded in lichen thalli; teleomorph filamentous, rarely observed; when fertile, basidia develop thick-walled probasidium and thin-walled, cylindrical meiosporangium; anamorph is the prevalent known form, consisting of budding yeast with round, thin-walled cells, 2.5 to 4.5 μm in diameter, embedded in the upper cortex of lichens, especially Parmeliaceae; exogenous compound utilization not characterized; cell wall constituents unknown. Type genus, *Cyphobasidium* Millanes, Diederich, and Wedin, *Fungal Biology* doi:10.1016/j.funbio.2015.12.003, p. 4 (2015).
20. M. E. Hale Jr., *Lichenologist* **13**, 1–10 (1981).
21. A. Thell *et al.*, *Nord. J. Bot.* **30**, 641–664 (2012).
22. A. Crespo *et al.*, *Taxon* **59**, 1735–1753 (2010).
23. C. L. Schoch *et al.*, *Proc. Natl. Acad. Sci. U.S.A.* **109**, 6241–6246 (2012).
24. E. Kalle, M. Kubista, C. Rensing, *Biomol. Detect. Quantif.* **2**, 11–29 (2014).
25. R. Honegger, "The symbiotic phenotype of lichen-forming ascomycetes and their endo- and epibionts," in *Fungal Associations*, B. Hock, Ed., vol. IX of *The Mycota*, K. Esser, Ed. (Springer, ed. 2, 2012), pp. 287–339.
26. D. Anglesea, C. Veltkamp, G. H. Greenhalgh, *Lichenologist* **14**, 29–38 (1982).
27. E. S. Olafsdottir, K. Ingólfsdottir, *Planta Med.* **67**, 199–208 (2001).
28. C. G. Boluda, V. J. Rico, A. Crespo, P. K. Divakar, D. L. Hawksworth, *Lichenologist* **47**, 279–286 (2015).
29. N. Arnold, W. Steglich, H. Besl, *Z. Mykol.* **62**, 69–73 (1996).
30. W. L. Culberson, *Taxon* **10**, 161–165 (1961).

ACKNOWLEDGMENTS

This project was supported by an incubation grant from the University of Montana to J.P.M. and T.S.; by an Austrian Science Fund grant (P25237) to T.S., H.M., and P.R.; by NSF (IOS-1256680, IOS-1553529, and EPSCoR award NSF-IIA-1443108) and NASA Astrobiology Institute (NNA15BB04A) grants to J.P.M.; by a NSF Graduate Research Fellowship (DGE-1313190) to D.V.; by a grant from the Swedish University of Agricultural Sciences Council for Ph.D. Education (2014.3.2.5-5149) to V.T.; and by a grant (DO2011-0022) from Stiftelsen Oscar och Lili Lamms minne to G.T. Specimens from Glacier Bay National Park, Alaska, were collected with the support of the U.S. National Park Service as part of CESU (Cooperative Ecosystem Studies Units) project P11AC90513. We thank D. Armaleo and F. Lutzoni of Duke University for allowing us to use unpublished data from the *Cladonia grayi* proteome, as well as P. Dyer, P. Crittenden, and D. Archer (University of Nottingham, UK) for access to unpublished data from the *Xanthoria parietina* genome project, which is conducted together with the U.S. Department of Energy Joint Genome Institute (supported by the Office of Science of the U.S. Department of Energy under contract no. DE-AC02-05CH11231). We thank T. Goward, M. Grube, P. Lukasik, J. T. Van Leuven, F. Fernández-Mendoza, A. Millanes, V. Wagner, and M. Wedin for discussions and L. Bergström, C. Gueidan, J. Hermansson, H. Holien, B. Kanz, E. Lagostina, S. Leavitt, B. McCune, J. Nascimbene, C. Printzen, T. Wheeler, and D. Winston for field support and fresh material. C. Björk, S. Gunnarsson, L. Herritt, M. Hiltunen, W. Obermayer, A. de los Ríos, and E. Timdal provided technical help, advice, and photos. We acknowledge the Purdue University Genomic Core Facility for generating transcriptomic data for

Downloaded from http://science.sciencemag.org/ on August 31, 2016

Cystobasidium minutum and the Institute of Molecular Biosciences–Graz Microscopy Core Facility and S. Kohlwein for providing infrastructural support for imaging. Data are available under accession numbers SRP076577 and SRP073687 in the National Center for Biotechnology Information (NCBI) Sequence Read Archive (transcriptomes), NCBI nucleotide accession numbers KU948728 to KU948928 (single-locus DNA sequences), and the Dryad digital repository at http://dx.doi.org/10.5061/dryad.7qv72 (alignments, scripts, and tree files).

SUPPLEMENTARY MATERIALS

www.sciencemag.org/content/353/6298/488/suppl/DC1
Materials and Methods
Figs. S1 to S16
Tables S1 to S12
References (*31*–*74*)
Movies S1 and S2

6 April 2016; accepted 22 June 2016
Published online 21 July 2016
10.1126/science.aaf8287

INFECTION

Increased plasmid copy number is essential for *Yersinia* T3SS function and virulence

He Wang,[1,2] Kemal Avican,[1,2] Anna Fahlgren,[1] Saskia F. Erttmann,[1,2] Aaron M. Nuss,[3] Petra Dersch,[3] Maria Fallman,[1,2] Tomas Edgren,[1]*† Hans Wolf-Watz[1,2]*†

Pathogenic bacteria have evolved numerous virulence mechanisms that are essential for establishing infections. The enterobacterium *Yersinia* uses a type III secretion system (T3SS) encoded by a 70-kilobase, low-copy, IncFII-class virulence plasmid. We report a novel virulence strategy in *Y. pseudotuberculosis* in which this pathogen up-regulates the plasmid copy number during infection. We found that an increased dose of plasmid-encoded genes is indispensable for virulence and substantially elevates the expression and function of the T3SS. Remarkably, we observed direct, tight coupling between plasmid replication and T3SS function. This regulatory pathway provides a framework for further exploration of the environmental sensing mechanisms of pathogenic bacteria.

Three human pathogenic *Yersinia* strains—*Y. pestis*, *Y. enterocolitica*, and *Y. pseudotuberculosis*—share a common 70-kb virulence plasmid (IncFII) that encodes a set of virulence proteins called Yops (*Yersinia* outer proteins) (*1*, *2*). These bacterial toxins are secreted by a plasmid-encoded organelle, the *ysc/yop* type III secretion system (T3SS) (*3*–*5*). The T3SS comprises ~20 proteins that span the inner and outer bacterial membranes (*6*, *7*). Upon contact with eukaryotic cells, *Yersinia* deploys the T3SS to translocate Yops into the cytoplasm of target cells via a translocon formed in the cell membrane (*8*, *9*). This process is strictly regulated, and Yop expression and secretion increase after the bacterium establishes intimate contact with the eukaryotic target cell (*10*). This cell contact–dependent regulation can be mimicked in vitro at 37°C by depleting Ca^{2+} from the growth medium (*11*).

Incubation of *Yersinia* at 37°C in Ca^{2+}-deficient medium leads to T3SS induction and growth restriction after approximately two generations (*4*). Growth arrest may be due to the metabolic burden caused by excess expression of plasmid-encoded T3SS proteins (*12*). Thus, the function of the T3SS is paradoxical, because conditions that promote Yop secretion result in bacterial growth restriction. This feature is incompatible with infection; consequently, we reasoned that *Yersinia* must have evolved a mechanism to circumvent this problem. We observed that increased amounts of virulence plasmid DNA were recovered from wild-type *Y. pseudotuberculosis* cells grown under T3SS-inductive conditions relative to bacteria grown under T3SS-repressive conditions (fig. S1B). Therefore, we hypothesized that *Yersinia* may undergo rapid changes in gene expression by increasing and decreasing virulence plasmid copy numbers. Rapid changes in gene dose could adjust the T3SS output to trade off virulence costs and the pathogen's metabolic capacity to optimize growth.

To explore a potential connection between virulence and plasmid copy number, we first determined plasmid (pIBX) copy numbers in *Y. pseudotuberculosis* YpIII (YpIII/pIBX) (*13*) cultures under different conditions with a polymerase chain reaction (PCR)–free whole-genome sequencing approach (*14*). The depth of coverage (the number of times a nucleotide is read during the sequencing process) reflects the concentrations of chromosomal DNA and plasmid DNA molecules in the sample. We found that the pIBX copy number increased from ~1 to ~3 per chromosomal equivalent when conditions were repressive (26°C) or inductive (37°C, Ca^{2+}-free), respectively, to T3SS activity (Fig. 1A). At 37°C in the presence of Ca^{2+} (T3SS-repressive conditions), the copy number increased only modestly (1.6 per chromosomal equivalent). Similar differences in plasmid

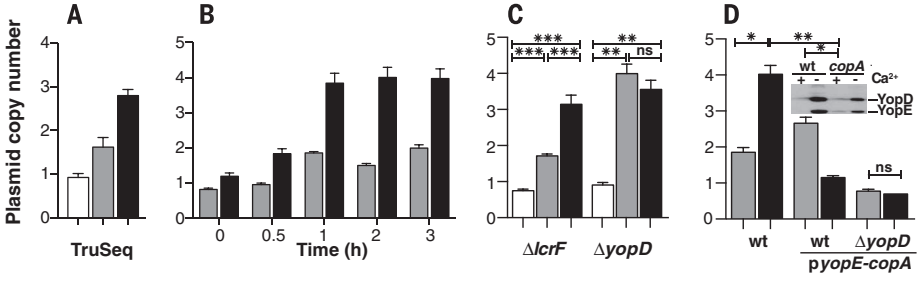

Fig. 1. *Y. pseudotuberculosis* differentially regulates virulence plasmid copy number in vitro. (**A**) Virulence plasmid copy numbers in DNA isolated from *Y. pseudotuberculosis* YpIII/pIBX grown for 3 hours under different conditions [white, 26°C; gray, 37°C under T3SS-repressive conditions (Ca^{2+}); black, 37°C under T3SS-inductive conditions] as determined by whole-genome sequencing (TruSeq). Copy number was calculated as the ratio of average depth of plasmid DNA coverage to chromosomal DNA coverage (N = 2). (**B**) Time course of plasmid copy number increase determined by qPCR. At time zero, *Y. pseudotuberculosis* cultures were shifted from 26° to 37°C under T3SS-repressive (gray) and T3SS-inductive (black) conditions. Plasmid copy number is defined as the number of plasmid equivalents per chromosome (N = 6). (**C**) Plasmid copy number changes in YpIII/pIB73 (Δ*lcrF*) and YpIII/pIB621 (Δ*yopD*) determined by qPCR after 3 hours of growth under the same conditions as in (A) (N = 6). (**D**) qPCR results showing plasmid copy numbers in YpIII/pIBX (wt) and a YpIII/pIB621 (Δ*yopD*) overexpressing the antisense *copA* RNA fused to the *yopE* promoter in cis (p*yopE-copA*) after 3 hours of growth at 37°C under T3SS-repressive (gray) and T3SS-inductive (black) conditions. Copy numbers in YpIII/pIBX (wt) are shown as control (N = 4). Inset: Immunoblot of whole-cell lysates from the indicated strains probed with antibodies to Yops. Data are means ± SEM (*$P \le 0.05$, **$P \le 0.01$, ***$P \le 0.001$, Mann-Whitney U test; ns, not significant).

[1]Umeå Centre for Microbial Research (UCMR), Department of Molecular Biology, Umeå University, SE-901 87 Umeå, Sweden. [2]Laboratory for Molecular Infection Medicine Sweden (MIMS), Department of Molecular Biology, Umeå University, SE-901 87 Umeå, Sweden. [3]Department of Molecular Infection Biology, Helmholtz Centre for Infection Research, Braunschweig, Germany.
***Corresponding author. Email: tomas.edgren@umu.se (T.E.); hans.wolf-watz@umu.se (H.W.-W.)** †These authors contributed equally to this work.

Downloaded from http://science.sciencemag.org/ on August 31, 2016

Basidiomycete yeasts in the cortex of ascomycete macrolichens
Toby Spribille, Veera Tuovinen, Philipp Resl, Dan Vanderpool, Heimo Wolinski, M. Catherine Aime, Kevin Schneider, Edith Stabentheiner, Merje Toome-Heller, Göran Thor, Helmut Mayrhofer, Hanna Johannesson and John P. McCutcheon (July 21, 2016)
Science **353** (6298), 488-492. [doi: 10.1126/science.aaf8287]
originally published online July 21, 2016

Editor's Summary

Lichens assemble in three parts

Lichen growth forms cannot be recapitulated in the laboratory by culturing the plant and fungal partners together. Spribille *et al*. have discovered that the classical binary view of lichens is too simple. Instead, North American beard-like lichens are constituted of not two but three symbiotic partners: an ascomycetous fungus, a photosynthetic alga, and, unexpectedly, a basidiomycetous yeast. The yeast cells form the characteristic cortex of the lichen thallus and may be important for its shape. The yeasts are ubiquitous and essential partners for most lichens and not the result of lichens being colonized or parasitized by other organisms.

Science, this issue p. 488

This copy is for your personal, non-commercial use only.

Article Tools Visit the online version of this article to access the personalization and article tools:
http://science.sciencemag.org/content/353/6298/488

Permissions Obtain information about reproducing this article:
http://www.sciencemag.org/about/permissions.dtl

Science (print ISSN 0036-8075; online ISSN 1095-9203) is published weekly, except the last week in December, by the American Association for the Advancement of Science, 1200 New York Avenue NW, Washington, DC 20005. Copyright 2016 by the American Association for the Advancement of Science; all rights reserved. The title *Science* is a registered trademark of AAAS.

Downloaded from http://science.sciencemag.org/ on August 31, 2016